ICANS-VI
INTERNATIONAL COLLABORATION ON ADVANCED NEUTRON SOURCES
June 27 - July 2, 1982

# POSSIBLE USE OF COPPER SPALLATION REACTIONS TO MEASURE HIGH ENERGY PARTICLE SPECTRA IN SHIELDING EXPERIMENTS

W. Amian, V. Drüke, M. Kloda, W. Litzow

Institut für Reaktorentwicklung
Kernforschungsanlage Jülich GmbH
Postfach 1913
D-5170 Jülich 1, Germany

## ABSTRACT

The formation of spallation products in copper foils has been used to derive the high energy part of the neutron energy spectra from spallation reactions. Spectra for lead and uranium spallation targets have been measured. The method allows to derive the neutron energy spectra by unfolding of the measured residual nuclei in the energy region of 100 MeV up 650 MeV with reasonable precision, which is illustrated by the confidence limits of the neutron spectra derived.

# POSSIBLE USE OF COPPER SPALLATION REACTIONS TO MEASURE HIGH ENERGY PARTICLE SPECTRA IN SHIELDING EXPERIMENTS

W. Amian, V. Drüke, M. Kloda, W. Litzow

Institut für Reaktorentwicklung
Kernforschungsanlage Jülich GmbH
Postfach 1913
D-5170 Jülich 1, Germany

## INTRODUCTION

Experiments have been performed to measure the formation of spallation products in copper foils by high energy neutrons emerging from thick cylindrical spallation targets of lead and uranium, respectively, bombarded by 1100 MeV protons. In addition "normal" threshold reaction foils have been used. While these reactions cover the energy region between about 1 MeV and 20 MeV, the copper spallation reactions have thresholds upto about 100 MeV. The cross sections for the "normal" threshold reactions have been taken from /1/, those for the copper spallation reactions are known only from calculations /2/. The unfolding of the measured activities has been performed with the code LOUHI78 /3/ to derive the neutron energy spectrum.

## EXPERIMENTAL

The copper foils and "normal" threshold reaction foils were about 10 cm downstream from the beam entrance to the target (rectangular parallelepiped of 15 x 15 x 90 $cm^3$) immediately on the target surface. The protonbeam of 1100 MeV energy had 11.2 nA intensity for the uranium target, 22.5 nA for the lead target, respectively. The formation of Fe59, Co58, Co57, Co56, Mn52, V48, Sc46 and Sc44 in the copper foils and of the respective isotopes in the "normal" threshold foils has been measured by gamma-ray spectrometry using Ge(Li)-detectors. Table I gives the saturation activities in units of decays per second per detector nucleus per proton.

The copper foils have been measured about three hours after the end of bombardment and afterwards about three months later. This explains why Cr48 and Na24 which have relatively long halflifes and low production cross sections have not been observed. Later experiments should reveal their existence by counting at intermediate cooling times. Strong overlapping activities at short times (hours) stem from Cu61, Mn56, Ni65, Cu64.

## RESULTS AND DISCUSSION

The spallation yield cross sections of different products for copper as calculated according to the Rudstam formulas /2/ are presented in figure 1. In the case of the "normal" threshold reactions, the cross sections have been set to zero above the highest energy known from the literature /1/.

The unfolding of the neutron energy spectra measured with the copper spallation reactions and the "normal" threshold reactions has been performed with the code LOUHI78. The comparison of the measured activities and the ones calculated for the spectrum derived are given in tables II and III, respectively.

The agreement of measured and calculated saturation activities is fairly well. However, since the product yield cross sections for the copper spallation reactions are not very well known this reasonable agreement has to be expected. Figure 2 gives the unfolded spectrum in units of neutrons per $cm^2$ per second per MeV and per proton for the uranium target, figure 3 for the lead target.

The confidence bands reveal that only the regions between 3 MeV and 15 MeV and between 100 MeV and 650 MeV can be unfolded with sufficient precision. This uniquely corresponds to the regions, where the cross sections dominantly contribute to the reactions observed. Further reactions with lower and higher thresholds are needed to get detailed information outside these regions.

## REFERENCES


/1/ D.I. Garber, R.R. Kinsey
Neutron Cross Sections, Volume II, Curves
BNL 325, Brookhaven National Laboratory (1976)

/2/ G. Rudstam
Z. Naturforschung 21 a (1966) 1027

/3/ J.T. Routti, J.V. Sandberg
Computer Physics Communications 21(198) 119

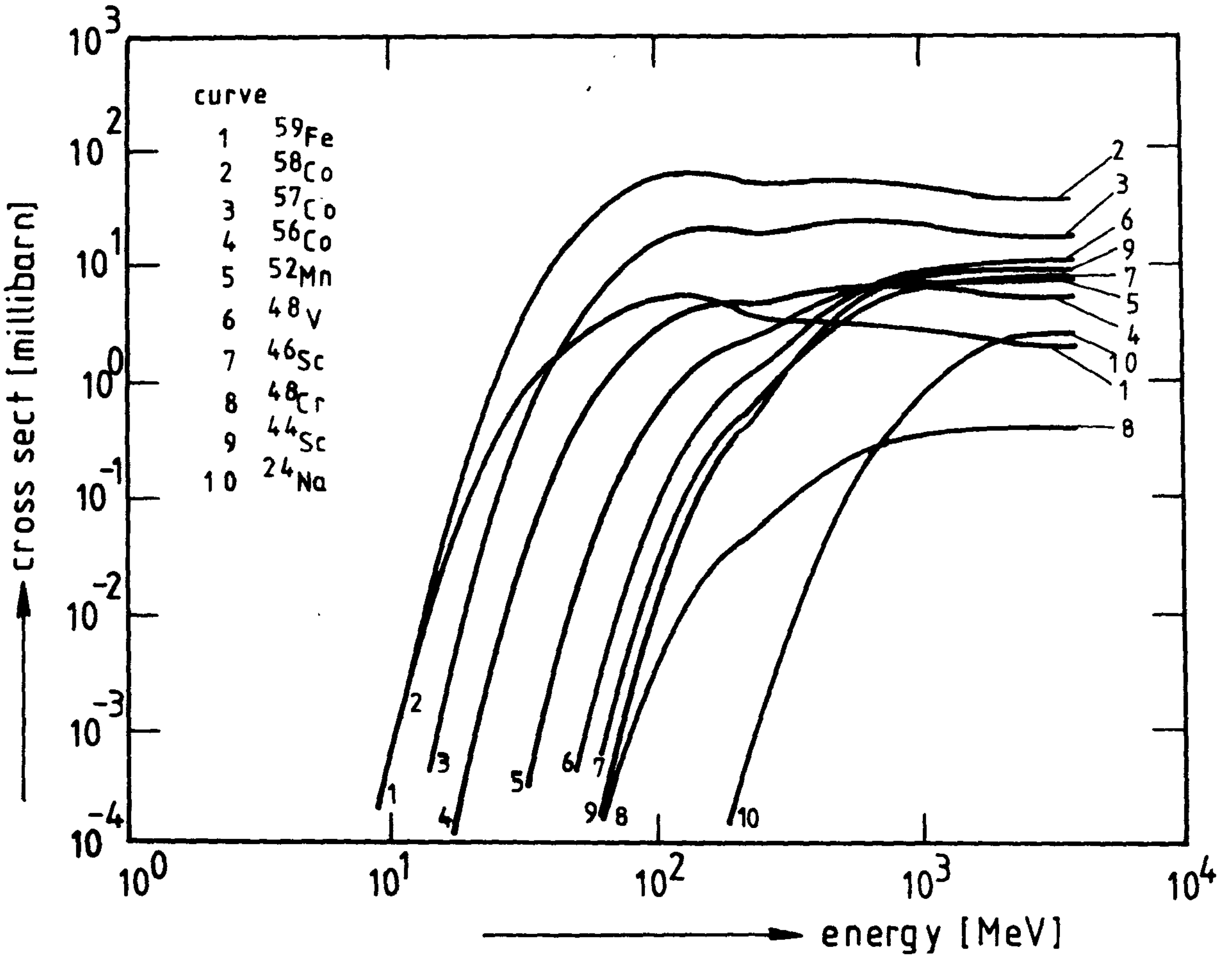


Fig. 1: Calculated spallation cross sections for copper

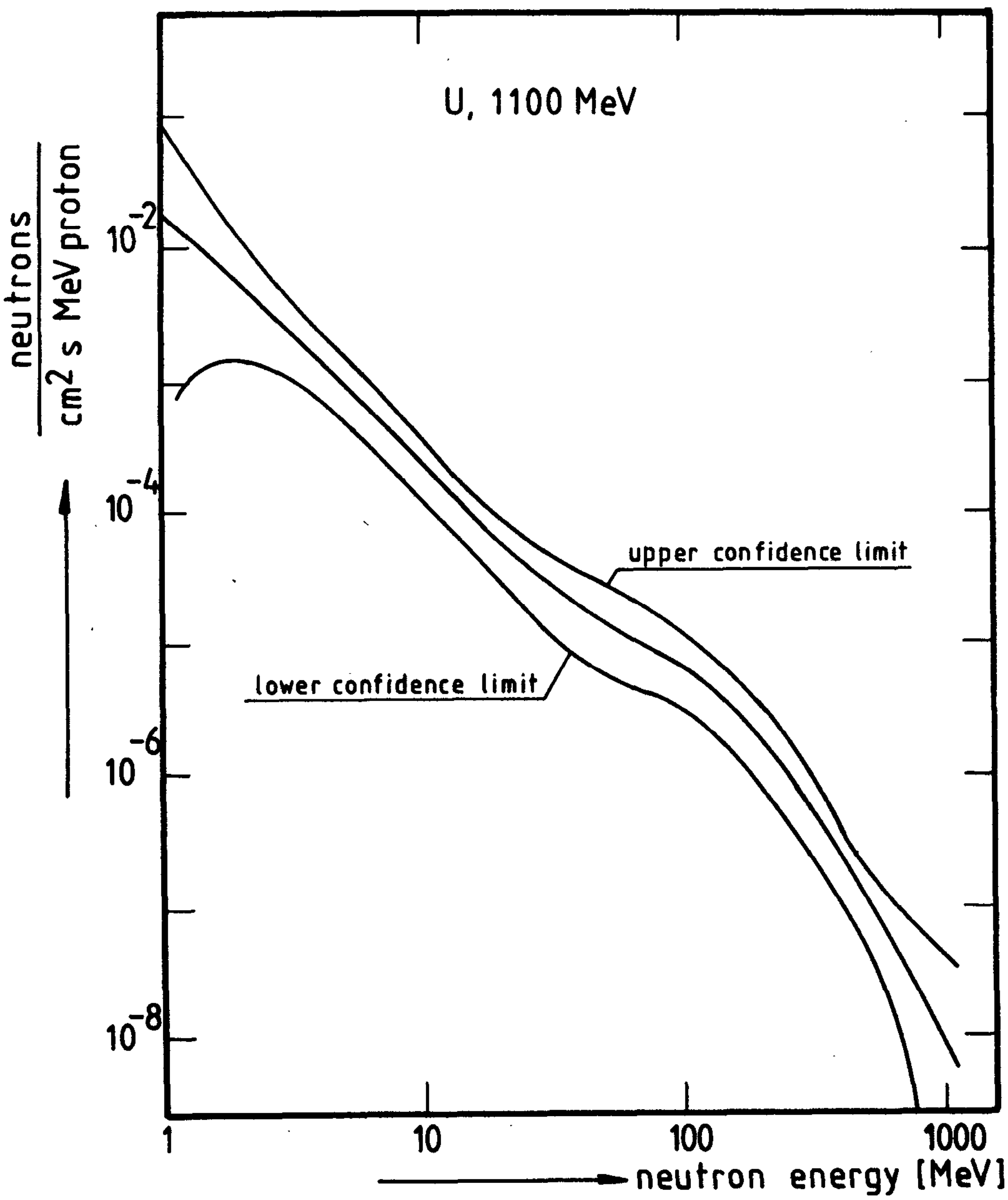


Fig. 2: Unfolded neutron energy spectrum at the surface, 10 cm from beam entry, for a rectangular uranium target (15 x 15 x 90 $cm^3$) at 1100 MeV

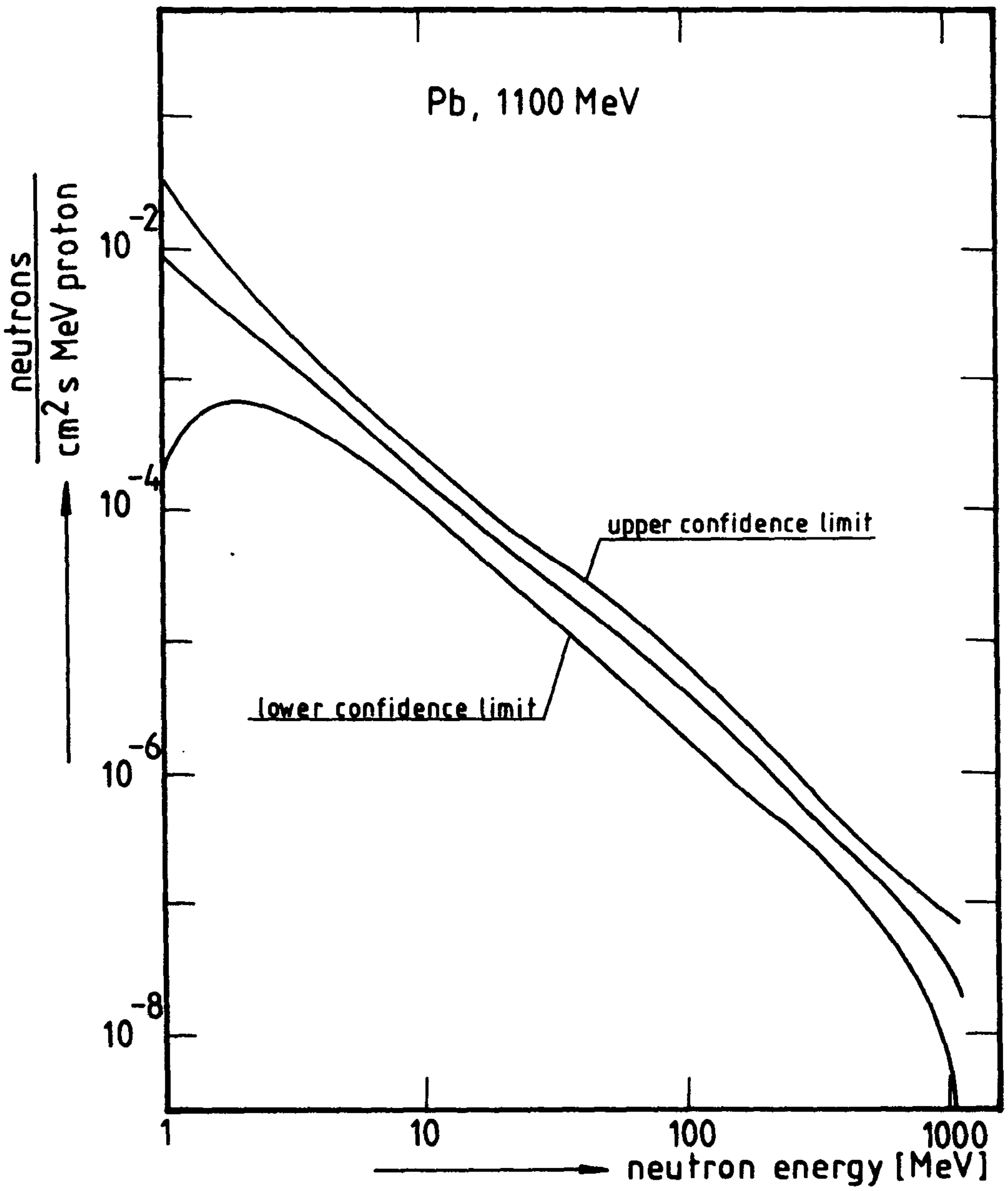


Fig. 3: Unfolded neutron energy spectrum at the surface, 10 cm from beam entry, for a rectangular lead target (15 x 15 x 90 $cm^3$) at 1100 MeV

| Nuclide | Halflife | Gamma-Energy (keV | Saturation Activity ($sec^{-1}$/proton/nucleus) Uranium | Lead |
|---|---|---|---|---|
| Fe59 | 45.1 d | 1099.22;1291.56 | 3.9 $10^{-30}$ | 3.3 $10^{-30}$ |
| Co58 | 70.78 d | 811.75 | 5.1 $10^{-29}$ | 4.9 $10^{-29}$ |
| Co57 | 270.00 d | 122.07; 136.43 | 2.7 $10^{-29}$ | 2.9 $10^{-29}$ |
| Co56 | 77.30 d | 846.75;1238.28 | 3.6 $10^{-30}$ | 4.2 $10^{-30}$ |
| Mn52 | 5.70 d | 1434.30; 935.60 | 2.0 $10^{-30}$ | - |
| V48 | 16.10 d | 983.50;1311.60 | 7.7 $10^{-31}$ | 9.4 $10^{-31}$ |
| Sc46 | 83.85 d | 1120.52; 889.26 | 4.4 $10^{-31}$ | 6.6 $10^{-31}$ |
| Sc44 | 3.93 h | 1156.95; | 2.2 $10^{-31}$ | 2.8 $10^{-31}$ |
| Cr48 | 23.00 h | 306.00; 116.00 | - | - |
| Na24 | 15.03 h | 1368.55;2754.10 | - | - |

Table I: Saturation activities for the copper spallation products produced from neutrons emerging from lead and uranium spallation targets, respectively

| Reaction | Saturation Activity ($sec^{-1}$/proton/nucleus) Measured | Calculated | % Difference |
|---|---|---|---|
| Cu(n,sp)Fe59 | 3.9 $10^{-30}$ | 5.1 $10^{-30}$ | 32.2 |
| Cu(n,sp)Co58 | 5.1 $10^{-29}$ | 5.1 $10^{-29}$ | 1.2 |
| Cu(n,sp)Co57 | 2.7 $10^{-29}$ | 1.5 $10^{-29}$ | 44.2 |
| Cu(n,sp)Co56 | 3.6 $10^{-30}$ | 3.1 $10^{-30}$ | 14.6 |
| Cu(n,sp)Mn52 | 2.0 $10^{-30}$ | 1.1 $10^{-30}$ | 43.8 |
| Cu(n,sp)V48 | 7.7 $10^{-31}$ | 5.5 $10^{-31}$ | 28.7 |
| Cu(n,sp)Sc46 | 4.4 $10^{-30}$ | 3.2 $10^{-30}$ | 26.4 |
| Cu(n,sp)Sc44 | 2.2 $10^{-30}$ | 3.0 $10^{-30}$ | 40.8 |
| Fe54(n,p)Mn54 | 5.8 $10^{-27}$ | 2.7 $10^{-27}$ | 53.7 |
| In115(n,n')In115m | 4.7 $10^{-27}$ | 4.8 $10^{-27}$ | 1.5 |
| Ni58(n,p)Co58 | 2.9 $10^{-27}$ | 3.5 $10^{-27}$ | 18.8 |
| Co59(n,$\alpha$)Mn56 | 5.4 $10^{-29}$ | 4.1 $10^{-29}$ | 25.4 |
| Nb93(n,2n)Nb29m | 3.5 $10^{-28}$ | 3.9 $10^{-28}$ | 14.6 |
| Zr90(n,2n)Zr89 | 1.1 $10^{-27}$ | 1.1 $10^{-27}$ | 3.3 |

Table II: Saturation activities of the reactions observed in comparison to the calculated saturation activities for the uranium target at 1100 MeV proton energy

| Reaction | Saturation Activity (sec$^{-1}$/proton/nucleus) Measured | Calculated | % Difference |
|---|---|---|---|
| Cu(n,sp)Fe59 | 3.3 $10^{-30}$ | 3.9 $10^{-30}$ | 17.3 |
| Cu(n,sp)Co58 | 4.9 $10^{-29}$ | 3.9 $10^{-29}$ | 20.9 |
| Cu(n,sp)Co57 | 2.9 $10^{-29}$ | 1.1 $10^{-29}$ | 60.5 |
| Cu(n,sp)Co56 | 4.2 $10^{-30}$ | 2.4 $10^{-30}$ | 43.2 |
| Cu(n,sp)V48 | 9.4 $10^{-31}$ | 6.2 $10^{-31}$ | 34.3 |
| Cu(n,sp)Sc46 | 6.6 $10^{-31}$ | 4.0 $10^{-31}$ | 39.5 |
| Cu(n,sp)Sc44 | 2.8 $10^{-31}$ | 4.2 $10^{-31}$ | 48.9 |
| Fe54(n,p)Mn54 | 4.5 $10^{-27}$ | 1.7 $10^{-27}$ | 62.3 |
| In115(n,n')In115m | 2.9 $10^{-27}$ | 2.7 $10^{-27}$ | 7.3 |
| Ni58(n,p)Co58 | 1.8 $10^{-27}$ | 2.2 $10^{-27}$ | 21.7 |
| Co59(n,$\alpha$)Mn56 | 4.2 $10^{-29}$ | 3.4 $10^{-29}$ | 18.8 |
| Nb93(n,2n)Nb29m | 2.8 $10^{-28}$ | 3.4 $10^{-28}$ | 21.8 |
| Zr90(n,2n)Zr89 | 1.0 $10^{-27}$ | 1.1 $10^{-27}$ | 10.0 |

Table III: Saturation activities of the reactions observed in comparison to the calculated saturation activities for the lead target at 1100 MeV proton energy